X-ray confinement in a gold cavity heated by 351-nm laser light

H. Nishimura, Y. Kato, H. Takabe, T. Endo, K. Kondo, H. Shiraga,
S. Sakabe, T. Jitsuno, M. Takagi, C. Yamanaka,* and S. Nakai
Institute of Laser Engineering, Osaka University, Suita Osaka, 565 Japan

R. Sigel, G. D. Tsakiris, J. Massen, M. Murakami,† F. Lavarenne, R. Fedosejevs,‡
J. Meyer-ter-Vehn, K. Eidmann, and S. Witkowski
Max-Planck-Institute für Quantenoptik, D-8046 Garching, Federal Republic of Germany
(Received 1 April 1991)

Thermal x-ray confinement in a laser-heated gold cavity was investigated. Intense blue laser light (wavelength 351 nm, energy 5 kJ, duration 0.9 ns) irradiated the inner surface of (1–3)-mm-diam gold shells at average intensities up to 2×10^{14}W/cm^2 to generate the source x ray for the confinement. A maximum brightness temperature of 240 eV and a quality factor of confinement of $N=5.3$ (corresponding to a reemission coefficient of $r=0.84$) have been achieved. Experimental results are in satisfactory agreement with theoretical predictions based on the self-similar ablative heat wave driven by radiation and with numerical simulations.

PACS number(s): 32.30.Rj, 44.40.+a, 52.25.Nr, 52.50.Jm

I. INTRODUCTION

The possibility of generating intense thermal radiation by modern pulsed power sources enables us to investigate phenomena of radiation hydrodynamics in a new range of temperature and density in the laboratory. An effective way to generate intense radiation is to utilize the radiation confinement effect in a cavity: If, for example, one or several beams from a high-power laser are introduced through small holes into a cavity made of high-Z material, they will generate a hot laser-produced plasma on the laser-irradiated parts of the wall. This plasma acts as a converter of laser light and represents a strong source of soft x rays inside the cavity. The x rays from this source provide so-called indirect heating of the total inner wall of the cavity including in particular those parts which are not directly heated by the laser light. The confinement effect arises because the cavity wall heats up due to the heating from this source and becomes itself a strong emitter of thermal soft-x-ray radiation. In this way a fraction of the flux which the wall receives from the source is reemitted into the cavity.

As a consequence of reemission an indirectly heated wall element receives radiation not only from the source but also remitted radiation from the other wall elements in the cavity. In this way it can radiate into the cavity a flux of thermal x rays which may exceed the received source flux. If the reemission coefficient of the hot-wall material reaches a value of order unity, a large circulating flux of reemitted radiation forms in the cavity which, for a wall emitting Planck radiation, is connected with a correspondingly high temperature through the Stefan-Boltzmann law. The spatial redistribution of the source energy connected with the existence of a large flux of reemitted photons will help to establish a spatially uniform temperature in the cavity. This feature is of great importance for applications where a high degree of spatial uniformity is required, for example in inertial confinement fusion.

The key element for describing the radiation confinement in the cavity is the reemission coefficient of the x-ray heated wall. It is determined by the radiation-driven ablative heat wave propagating into the depth of the wall material. Pakula and Sigel [1] have extended the self-similar solution of a radiation-driven heat wave first given by Marshak [2] to include expansion of the heated material which is important for the conditions achievable with laboratory pulsed power sources. The necessary opacities for high-Z material have been calculated by Tsakiris and Eidmann [3]. Based on the scaling of the self-similar solution one expects that the reemission coefficient increases with the power of the source and that with presently available lasers conditions may be achieved where the flux of reemitted radiation from an indirectly heated wall element exceeds the flux received from the plasma source in the cavity.

There have been several experimental investigations of x-ray confinement in cavities heated by lasers [4–7]. A brightness temperature of up to 190 eV and a reemission coefficient of the wall of 0.5 were achieved with high-power green laser light [7]. However, these experiments suffer, to some extent, from application of relatively long-wavelength laser light. In this case, due to high temperatures, the laser-produced plasma expands rapidly during laser irradiation thus filling the cavity void. It carries a large fraction of the laser energy because for such long-wavelength light the conversion of laser light into source x rays is low. This plasma contributes to the radiation from the cavity wall when it is observed through a small diagnostic hole [8,9] and complicates the comparison with simple models based on the ablative heat wave in which an empty cavity is assumed. Also a not precisely known but considerable fraction of laser radiation may be reflected from the laser-irradiated area in-

side the cavity, making it difficult to distinguish between laser-heated and purely x-ray-heated wall elements. Another serious complication arises from the fact that the hot plasma filling the cavity becomes an extended target plasma for the laser light. This may lead to nonlinear laser-plasma coupling with the consequence of fast electron generation [10,11]. Thus the generation of intense thermal radiation under "clean" conditions, where only the thermal radiation field is present in the vacuum of the empty cavity, was difficult to achieve in these experiments.

In this paper, we shall present an experimental study of x-ray confinement in laser-heated cavities. The major differences to the previous studies are the following: (i) Short-wavelength laser light (351 nm) was employed for cavity heating; (ii) large cavities with diameters up to 3 mm were used; and (iii) the effect of openings in the cavity on radiation confinement was studied.

We note that (i) and (ii) are essential for the generation of clean conditions in the cavity. At the short-wavelength employed efficient laser light, absorption [12] of ≥ 0.9 and a large conversion rate of absorbed laser light into x rays [13,14] of ≥ 0.5 can be expected. Especially in the large cavities this should lead to the realization of cleaner conditions than before.

Following a short description of analytical modeling of x-ray confinement based on the self-similar solution (this is called the similarity model in the following) in Sec. II and a discussion of the experiment in Sec. III, we shall present a comparison of the experimental results with theoretical predictions and with one-dimensional (1D) hydrodynamic code calculations in Sec. IV. A summary of the main results is given in Sec. V. We note that a short account of the present work has been given elsewhere [15].

II. SIMILARITY MODEL FOR X-RAY CONFINEMENT

Quantitative modeling of the injection of several laser beams into the cavity, the subsequent conversion of the laser light into soft x rays, and the resulting spatial distribution of energy deposition would meet considerable difficulties, owing to the complicated geometry and the rather involved physics of laser light conversion. In order to arrive at a tractable model we therefore replace the laser simply by a fictitious source of x rays, located inside the cavity but occupying a negligible fraction of the cavity wall. It is assumed that the power of this source can be calculated from the known power injected into the cavity, by making an assumption about the conversion efficiency into soft x rays (see Sec. IV). In addition, we assume that radiation and matter are in complete thermodynamic equilibrium in the cavity, i.e., the wall emits Planck radiation into cavity and the loss of energy by diffusion of radiation into the wall can be calculated in the approximation of radiation heat conduction. The analytical model which follows from these assumptions and which is discussed in the following is based on the self-similar solution for the radiation heat wave [1,6] which forms in the cavity wall.

Consider a wall element of a cavity which receives a flux S_s from the source and an incident flux S_i of thermal radiation from the other wall elements of the cavity. It is assumed that the hot-wall material is optically thick and that the received radiation is completely converted into blackbody radiation in a thin surface layer. This layer radiates a reemitted flux S_r into the cavity whereas a net heat flux $S_{\rm hw}$ of radiation diffuses into the wall. The quasistationary energy balance of this thin surface layer is given by $S_s+S_i=S_r+S_{\rm hw}$. We allow localized holes in the cavity with a fractional hole area n^{-1} but assume uniform energy distribution conditions in the cavity, i.e., the source flux is the same for all wall elements and the reemitted radiation from a wall element falls uniformly on all other wall elements including holes. Under this model assumption S_i and S_r are obviously related by [6]

$$S_i=(1-n^{-1})S_r \ . \tag{1}$$

It should be emphasized here that the assumption of uniform deposition of the source and reemitted photons is not an arbitrary one but would be fulfilled exactly in a spherical cavity (as used in our experiments) if the photons are emitted from the wall with an angular characteristic corresponding to a Lambertian radiator. This is a well-known property of a so-called Ulbricht or integrating sphere. The indirectly heated parts of the wall, reemitting Planck radiation from an optically thick layer of hot material, are indeed expected to radiate as a Lambertian radiator resulting in a perfectly uniform deposition in a spherical cavity. It is only for the source radiation, originating on the laser-irradiated parts of the wall, that the angular radiation characteristics are not well known and deviations from perfect uniformity must be admitted.

Together with the energy balance relation described above, Eq. (1) becomes

$$S_{\rm hw}=S_s-n^{-1}S_r \ . \tag{2}$$

For a given heat flux $S_{\rm hw}$ the temperature at the boundary between the ablation heat wave and the vacuum (which corresponds to the thin surface layer introduced above) is given by the self-similar solutions for the ablative heat wave in gold as [1,6]

$$T=3.11\times 10^6 \hat{S}_{\rm hw}^{4/13}\hat{t}^{2/13}\ ({\rm K}) \ . \tag{3}$$

where $\hat{S}_{\rm hw}$ and $\hat{t}$ are the heat flux expressed in units of 10^{14} W/cm^2 and the time in units of 10^{-9} s, respectively. In a completely closed cavity ($n^{-1}=0$) the source flux must flow into the wall (because there is no other loss than heat propagation into the wall) and the boundary condition for the heat wave is $S_{\rm hw}=S_s$. In this case the temperature can be directly calculated from Eq. (3) for a given source flux S_s. In a cavity with holes the situation is more complicated because some of the energy supplied by the source is lost through the holes in the form of reemitted radiation. However, as has been discussed in more detail in Ref. [6], Eq. (3) may be used to obtain approximate values for the temperature if $S_{\rm hw}$ is expressed through Eq. (2). Noting that for blackbody radiation $S_r=\sigma T^4$ (σ is the Stefan-Boltzmann constant), Eq. (3)

then becomes an implicit equation for the reemitted flux S_r, which can be readily solved. Thus S_r and T are obtained as a function of the given quantities n^{-1}, S_s, and t. With the help of S_r one finds the reemission coefficient r as

$$r\left[\equiv\frac{S_r}{S_s+S_i}\right]=\frac{S_r}{S_s+(1-n^{-1})S_r}\ , \tag{4}$$

where Eq. (1) has been used. Alternatively one may calculate the quality factor $N\equiv S_r/S_{\rm hw}$ which is related to r by $N=r/(1-r)$. In a closed cavity where $S_{\rm hw}=S_s$, N is equal to the ratio of the reemitted flux to the received source flux of the wall. Physically it corresponds to the number of reemissions of the source energy, inside the cavity. We may note that S_r and S_s are related through

$$S_r=\frac{S_s}{N^{-1}+n^{-1}}\ , \tag{5}$$

i.e., for a given source flux S_s the reemitted flux S_r (and correspondingly the temperature) depends in a similar manner on the losses which take place in the wall (represented by N^{-1}) and through the holes (represented by n^{-1}). Figure 1 shows the reemission coefficients for a closed cavity ($n^{-1}=0$) of gold, calculated in the manner described above, as a function of the source flux at different times. The reemission coefficients for open cavities are weakly dependent on the fractional hole area (because the wall becomes colder in more open geometry for a fixed source flux) and are smaller than the values shown in Fig. 1, for example, by about 1% for $n^{-1}=0.1$ and 5% for $n^{-1}=0.4$ at $t=0.9$ ns given as the experimental value. These fractional hole areas are representative values for the cavities employed in the experiment. The boundary between the solid and dashed lines shows a criterion from which in the lower source flux side the similarity model becomes gradually invalid (for more details see Sec. IV B). Reemission coefficients of 0.70–0.85 (the corresponding values for the quality factor are $N=3$–5) are expected for the parameter range of this study.

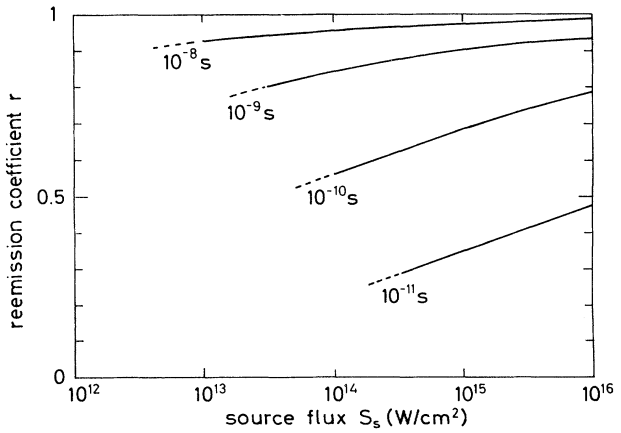

FIG. 1. The reemission coefficients of the wall of a closed cavity ($n^{-1}=0$) of gold, derived from Eqs. (2) and (3) as a function of the source flux at different times.

For more detailed consideration, a review of the generation of intense thermal radiation in laser-heated cavities has recently been given by Sigel [16].

III. EXPERIMENT

A. Laser

The cavities were irradiated with third-harmonic laser light (351 nm) from the Gekko XII Nd:glass laser facility [17]. Ten beams were used, forming two bundles of five beams from opposite sides. The bundles have a common horizontal axis with respect to which each beam makes an angle of 50°. The f number of the focusing lenses was 3.0. The laser-pulse shape at 351 nm was routinely monitored. The measured pulse shape was asymmetric (faster rise than decay) and can be approximated by

$$I(t)=I_L^{\rm peak}\exp\left[-\left|\frac{At}{\tau_m}\right|^{\alpha}\right]\ ,$$
$$m={\rm I}\ (t<0)\ \ {\rm or}\ \ {\rm II}\ (t\geq 0)\ , \tag{6}$$

where $\tau_{\rm I}$ is the width at half maximum of the rising part of the signal and $\tau_{\rm II}$ the decaying part [i.e., $\tau_{\rm I}+\tau_{\rm II}$ corresponds to the nominal full width at half maximum (FWHM)]. $I_L^{\rm peak}$ is the peak flux of incident laser at $t=0$. Typical values determined from the measurement were $A=0.853$, $\alpha=2.3$, $\tau_{\rm I}/\tau_{\rm II}=\frac{3}{5}$, and $\tau_{\rm I}+\tau_{\rm II}=0.87\pm0.04$ ns. The laser energy per beam was 358 ± 54 J. Errors of pulse shape and laser energy are due to shot-to-shot fluctuations.

B. Targets

The cavity targets used in this experiment are categorized into four types as illustrated in Fig. 2. Types A and D are standard single-shell cavities of spherical shape having laser inlet holes and diagnostic holes. Large openings were additionally made on the target D to increase the fractional hole area as much as possible. Although targets A and D are not completely closed or open, they will be hereafter called closed cavity and open cavity, respectively.

Target B is composed of three coupled cavities [18]. The central cavity is heated by the laser beams. X rays generated in this converter cavity can propagate through the connecting holes into the two satellite cavities and heat them. One of the satellite cavities is nearly closed and the other has large openings. In this way it is possible to investigate the effect of holes on radiation confinement by relative measurements between the two satellite cavities without disturbances from a laser-produced plasma. In this meaning this target may be called clean cavity. The details of this target and its experimental studies are given in Ref. [18]. Here we present only the results related to the emission from the converter cavity.

Target C is another type of clean cavity. This target differs from A in the way the laser light is coupled to the target. The five laser beams from one bundle encounter the first five cones that are made of the same material as

the cavity (gold). These cones were arranged in correspondence to the illumination geometry of the experimental facility and were built into the target. The laser beams heat the inside of the cones. Specularly reflected laser light (if generated at all in these short-wavelength irradiations) can reach the main cavity only after two reflections and, therefore, is largely absorbed. The primary x rays produced at the cones cannot reach the main cavity directly, which is thus heated only by reemitted x rays propagating through the gaps between the cones. In this way the central part of the cavity which carries the diagnostic holes is not exposed to direct radiation from the laser-irradiated area inside the cones.

In parallel, we also investigated the propagation of the radiation heat wave into the wall by observing the sharp onset of radiation from the outer surface of a thin foil incorporated into the wall of the cavity. The results of this investigation have been published [19] and will be discussed in more detail elsewhere [20].

The targets were spherical shells made of gold whose wall thickness was 10 μm. Cavity diameters varied from 1 to 3 mm to yield 7×10^{12}–2×10^{14} W/cm^2 average laser flux $\bar{S}_L$ (incident laser power divided by the surface area of the sphere with the diameter of the cavity). The diameters of the diagnostic holes were typically 450 μm (for 3-mm cavity), 200 μm (for 2-mm cavity), and 100 μm (for 1-mm cavity). The position of the diagnostic holes was determined with the aid of ray-tracing calculation for laser light in the cavity in such a manner that the wall element observed through a hole could be reached by laser light only after four specular reflections at the cavity wall (in which case the light is expected to be completely absorbed). Another criterion for the positioning of the diagnostic holes was to avoid observing direct radiation from the laser-produced plasma streaming to the center of the cavity [5]. Figure 3 (an example of the ray-tracing study) shows the position of the first, second, and third reflection of the light rays (denoted by 1, 2, and 3) on the inner surface of the cavity. As can be seen from this figure, the laser beams were focused in such a manner that their first bounce on the cavity wall occurred on the meridian with respect to which the two laser holes were symmetrically located. Correspondingly, the common focus point of the five beams of each bundle was located on the horizontal axis of the bundles (passing through the center of the laser holes) at a distance $h=R/\tan50^\circ=0.84R$ (where R is the cavity radius) from the center of the cavity.

Targets with diagnostic holes as well as laser inlet holes were made by means of a photolithographic technique. In a first step a massive mandrel with a shape corresponding to the cavity and its support was machined out of brass on a lathe. The mandrel was then electroplated with a 10-μm-thick layer of gold. Holes were made by overcoating the gold with positive photoresist, exposing the hole areas with uv light, removing the exposed photoresist, and etching the gold layer away on the hole areas. Then

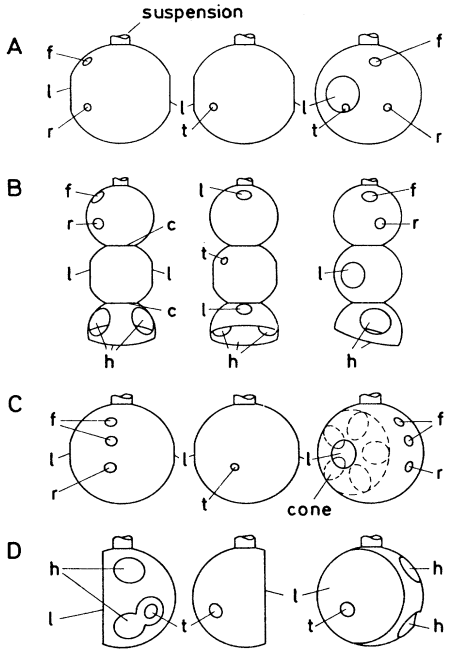

FIG. 2. Cavities of type A to D used in the experiments. Each target is shown in three different views, corresponding to rotation angles around the axis of suspension of $+90^\circ$ (left), -90° (middle), and $+30^\circ$ (right). Small letters denote the holes with foil (f) and the open reference hole (r) for the measurement of radiation heat wave (reported in Ref. [19]), the diagnostic hole for temperature measurement (t), the laser inlet holes (l), the connecting holes (c), and additional openings (h) in the open cavities.

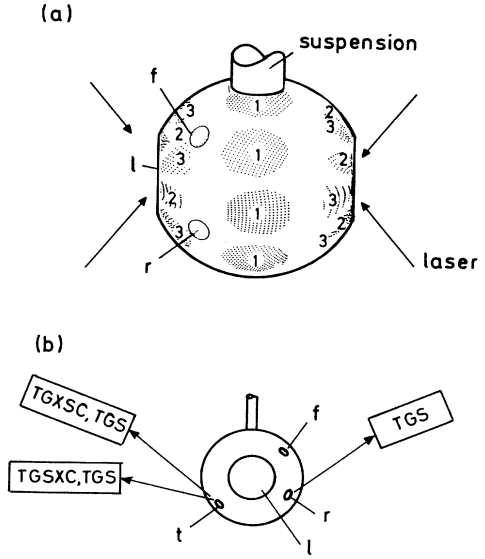

FIG. 3. (a) An example of the ray-tracing calculations for laser light for a type of type-A cavity. Numbers 1–3 denote the first, second, and third bounce of the laser light rays. (b) Three transmission grating spectrometers with film recording (TGS) and two identical spectrometers with x-ray streak cameras (TGXSC) were used to measure the radiation from the different wall elements at various observations angles.

the brass was leached out of the cavity through the holes. A laser light shield was attached at the edge of each laser inlet hole to prevent the outer surface of the cavity from being heated by the fundamental and the second-harmonic laser light from the laser system. The fractional hole areas n^{-1} were in the range 0.035–0.089 for the closed cavities and 0.37–0.39 for the open cavities.

C. Diagnostics

The main diagnostic instruments were transmission grating spectrometers with either an absolutely calibrated x-ray film [transmission grating spectrometer (TGS)] or an x-ray streak camera [transmission grating spectrometer with an x-ray streak camera (TGXSC)] as a detector. The free-standing gratings were made of 0.4-μm-thick gold with 1000 line pairs/mm and were mounted on a pinhole disk or on a slit. The pinhole diameters were 25 or 50 μm corresponding to a spatial resolution of about 50 or 100 μm. Spectral resolution was 0.2–0.4 nm mainly determined by the size of the diagnostic hole. The gratings used here were carefully selected with an electron microscope in order to avoid irregular dispersion and scattering of x rays due to grating imperfections. As the grating efficiency is known to be dependent upon the gap between the grating bars and upon the grating pitch [21], the efficiency of the first order was determined to be 0.10 from the microscope observation. Validity of determining the grating efficiency from the geometrical size has been confirmed by characteristic of transmission gratings with synchrotron radiation [22]. A 7.7-μm-thick Be filter was put in front of one of the pinhole gratings in order to suppress blurring of the spectra by soft x rays emitted during the cooling and expansion of the cavity. In this way it is possible to record very clear spectra in the range of 0.70 to 2.0 keV. X rays in this spectral range are emitted only when the cavity acquires high temperature and are therefore well suited to determine the maximum temperature in the cavity.

The recording film was Kodak type 101-01 or 101-07 soft-x-ray film. Absolute calibration of both films was performed by using a pulsed x-ray source from a laser-produced plasma [23,24]. The accuracy of the calibration was $\pm 25\%$.

The TGS measured the time-integrated fluence of x rays emanating from the inner wall of the cavity through the diagnostic hole per unit surface area at the cavity wall, per unit solid angle, and per unit energy as a function of the photon energy [14]. Assuming that the wall radiates like a Lambertian radiator (i.e., with a $\cos\theta$ angular distribution, where θ is the angle measured from the surface normal of the inner wall) and integrating over the observable spectral range of 0.1 to 2 keV, we obtained the time integral of the reemitted flux S_r of the observed wall element.

Slit gratings were used in combination with an x-ray streak camera in order to obtain time-resolved spectra with a time resolution of 30 ps. The jitter of the streak camera with respect to the laser pulse was measured to be less than ± 50 ps. The absolute spectral response of this system was calibrated using the time-integrated data from the TGS. In this way the reemitted flux S_r of the observed wall element was obtained and from it, using the Stefan-Boltzmann law, the brightness temperature as a function of time.

Three sets of TGS and two sets of TGXSC were used as schematically shown in Fig. 3(b). In addition to the observation of the wall emission through the diagnostic hole, a measurement was made at a different observation angle along the line of sight for which a large hole existed in the opposite wall of the cavity (see the left-hand-side representation of cavity D in Fig. 2). In this way it was attempted to measure volume emission from the interior of the cavity. The volume emission from open-cavity targets was found to be about 20% of the wall emission for all cavity diameters. Because this value is smaller than the errors of spectral measurements due to shot-to-shot fluctuations, the influence of volume emission on observed spectra is neglected in the following.

X-ray images were also taken with four pinhole cameras (XPHC's) with Be (50 μm thick), Al (7.5 μm), and Ti (5 μm) filters covering the spectral range from 1 to 4 keV. The pinhole cameras were mainly used to monitor whether all laser beams had been successfully injected into the cavity without hitting the edge of the laser inlet hole.

D. Experimental results

Figure 4 shows a soft-x-ray image taken with the TGS for the 1-mm closed cavity. Two spectral images are

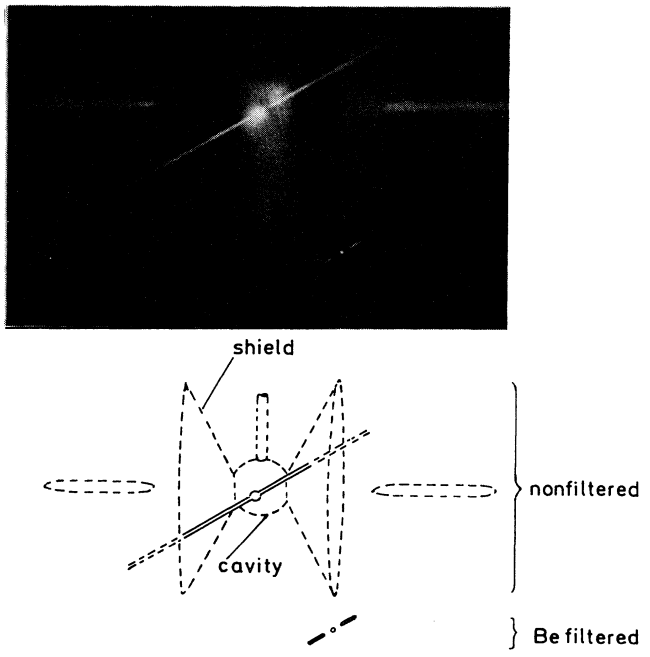

FIG. 4. A typical film image from TGS equipped with two pinhole gratings. The two spectra from the unfiltered (upper) and filtered (lower) pinhole gratings are superimposed on a pinhole image of the radiating cavity, produced in zeroth order by the unfiltered grating. Dispersion direction of the grating was tilted in order to avoid the spectra coinciding with the radiating plasma jets from the shields.

seen; one is from a TGS with no filter and the other is from a TGS with the Be filter. For the filtered spectrum a clear image with sharp boundaries corresponding to the edges of the diagnostic hole is obtained as mentioned above. A weak x-ray emission from the laser light shielder and plasma jets near the laser inlet holes are also seen. A 2D microdensitometer was used for data processing, and the background noise was subtracted from the original signal to obtain time-integrated spectra. Such spectra are shown in Fig. 5. Each spectrum is the average of the spectra obtained with the different spectrometers for the same laser irradiation. The time-averaged brightness temperatures for the Planckian spectra given in Fig. 5 were obtained from the radiated energy and the emission duration for each target. The radiated energy was determined from the time-integrated spectrum by integrating over the spectral range from 90 eV to 2.0 keV. The emission duration was determined from the FWHM value of the spectrally integrated emission signal provided by the streak camera. With decreasing cavity size the average laser flux and the temperature increase. Good agreement between the observed and the corresponding Planckian spectrum is obtained over most of the observed spectral range. Only in the low-energy region below 0.25 keV does the spectral intensity exceed the Planckian. This observation is tentatively attributed to the fact that in this time-integrated measurement the film also registers the very soft x rays emitted during the cooling phase of the cavity. As a result the spectrum in the low-energy region may exceed the Planckian for the average temperature, which is mainly determined by the x-ray emission in the heating phase.

The variation of the brightness temperature with time obtained from the streak data is shown in Fig. 6 for three experiments with cavities of (a) 3-mm, (b) 2-mm, and (c) 1-mm diam. A sharp rise and a slow decay of the temperature are seen. The maximum temperature rises with decreasing cavity size from 97 eV for the 3-mm cavity to 230 eV for the 1-mm cavity for the three representative shots shown in Fig. 6. The reemitted x-ray flux S_r at the time of the maximum temperature is plotted in Fig. 7 as a function of the incident laser flux for the different cavities. Each data point is an average of the temperatures over several (typically 3) identical target irradiations. Error bars represent the standard deviations from the average due to shot-to-shot variation. The highest temperature [see Fig. 7(a)] of 240±16 eV has been achieved in the 1-mm cavities of type *A*. For the target *B* (heated by six laser beams only) and for the open cavity *D* the temperatures are slightly lower as one might expect from the similarity model. A detailed discussion of these values is given in the following section.

IV. DISCUSSION

A. Comparison with the similarity model

Qualitative evidence for the importance of radiation confinement in the present experiment may be obtained

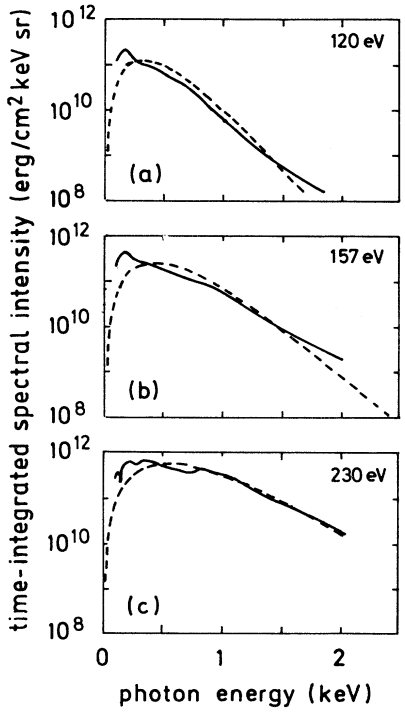

FIG. 5. Time integrated soft-x-ray spectra for (a) 3-mm, (b) 2-mm, and (c) 1-mm closed cavities of type *A*. The numbers in the upper right corners correspond to the time-averaged brightness temperature of the Planckian curves shown by the dashed lines.

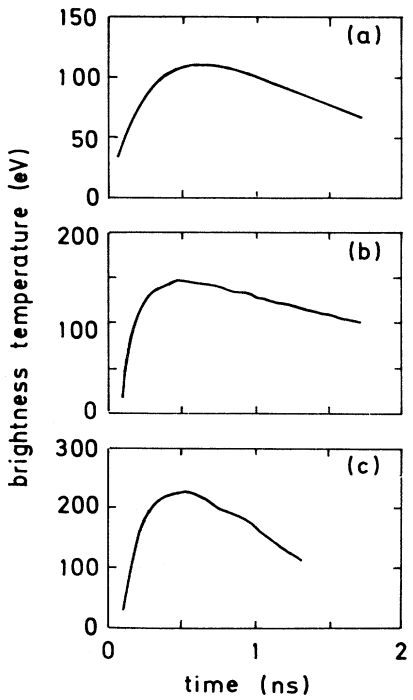

FIG. 6. Time evolution of the brightness temperature for (a) 3-mm, (b) 2-mm, and (c) 1-mm closed cavities of type *A*.

from Fig. 7 by observing that the experimental points (particularly those of the smallest, closed cavities) lie generally above the line $S_r = \bar{S}_L$, where $\bar{S}_L$ is the incident laser flux averaged over the whole inner surface area of the cavity wall. This means that the observed wall element emits more power in the form of thermal x rays than corresponds to its share of the available laser power. As was discussed in the Introduction, this is possible only if the observed wall element received additional heating from the other wall elements in the cavity. It should also be noted that the confinement effect is probably larger than might first appear from Fig. 7 because for an assessment of the confinement provided by the hot wall material the reemitted flux S_r should be compared to the source flux S_s rather than to the incident laser flux $\bar{S}_L$. S_s, however, is expected to be smaller than $\bar{S}_L$ because of incomplete conversion of laser light into x rays.

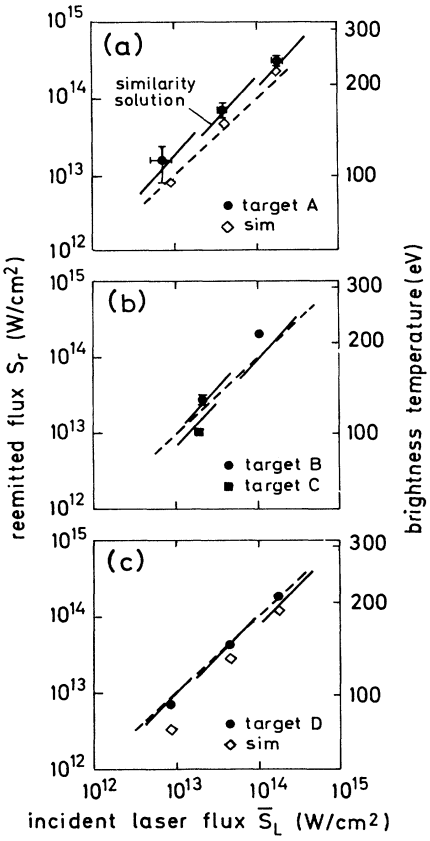

FIG. 7. (a) Reemitted flux S_r and corresponding brightness temperature measured with the cavities of type A of 3-, 2-, and 1-mm diam (from left to right) are plotted as a function of incident average laser flux $\bar{S}_L$. The predictions of the similarity model are represented by solid lines for each cavity size. On the dashed line where $S_r = \bar{S}_L$ the reemitted x-ray flux and the inner laser flux would be equal. Results from the 1D simulation are also indicated with open diamonds. (b) and (c) The same as above but for the central cavities of type B and C and for cavities D, respectively.

For a quantitative comparison with the similarity model (as described in Sec. II) we have obtained the source flux as $S_s = \eta_x S_L A_{\text{spot}} / A_{\text{cav}}$ $(= \eta_x \bar{S}_L)$. Here S_L is the actual laser intensity at the laser spot. A_{spot} and A_{cav} are, respectively, the areas of the laser spot and the whole cavity including holes. η_x is the overall conversion efficiency from the incident laser light into x rays, which is equivalent to the product of the absorption efficiency of the laser light η_{abs} and the conversion efficiency η_{con} of absorbed laser light into x rays. As is well known, the overall conversion efficiency is a function of laser irradiance. We assumed efficiencies suggested by measurements in open geometry [13,14] for laser intensities corresponding to those at the first bounce of the heating lasers. The assumed conversion efficiency η_x is 0.8 for the 3-mm-diam cavity, 0.7 for the 2-mm cavity, and 0.5 for the 1-mm cavity. For each cavity size the appropriate value of the fractional hole area n^{-1} was taken into account. For target C the efficiency of energy transfer by x rays into the central part of the cavity was estimated with the help of the same analysis of coupled cavities as described in Ref. [18]. The flux S_r and also the brightness temperature $T = (S_r/\sigma)^{1/4}$ were then evaluated as described in Sec. II at $t = 0.9$ ns (this time corresponding to the full width of the experimental laser pulse). The predicted value of S_r as a function of $\bar{S}_L$ is shown in Fig. 7 (solid lines) for each cavity size and type. The predicted curves differ slightly for each type of target because of the different input quantities n^{-1} and S_s.

As can be seen from Fig. 7, there is good overall agreement between experiment and theory over the very large parameter range covered in these experiments (the incident laser flux was varied by a factor of more than 20 and the measured brightness temperature changed by a factor of 2.3). This is taken as an indication that the model, despite the strong simplifications involved in it, gives basically a correct description of radiation confinement. Only in the smallest, most strongly heated cavities do the reemitted flux and the brightness temperature tend to be slightly higher than predicted. We shall discuss possible reasons for this behavior in connection with the numerical simulations.

Comparison between the experimental result and the prediction by the similarity model for the target C suggests that the emission from the main cavity (radiation confinement section) is indeed due to propagation of thermal radiation from the x-ray conversion section. Because of the low efficiency of energy coupling between the conversion section and the main cavity and the loss of radiation through the laser holes, the resultant reemitted flux is not as high as for a simple cavity with the same total area and the same hole fraction as the target C.

Another representation of the data of Fig. 7 is shown in Fig. 8. In this figure the flux enhancement S_r/S_s is plotted versus the fractional hole area n^{-1}. The closed and open cavities are represented by solid and open circles, respectively (the cavity sizes of 3-, 2-, and 1-mm diam are distinguished by the size of the symbols). Also shown are theoretical predictions for the three cavity sizes calculated with $S_s = 5.0 \times 10^{12}$, 2.6×10^{13}, and

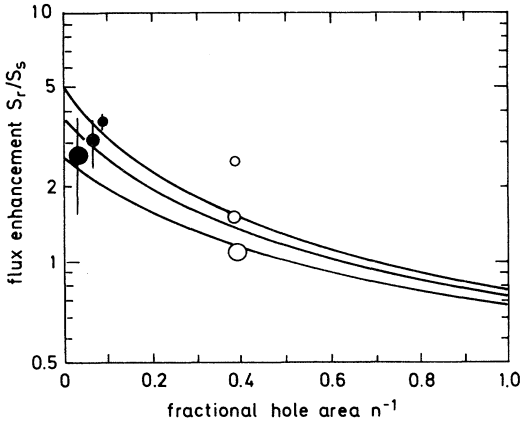

FIG. 8. X-ray flux enhancement S_r/S_s as a function of the fractional open area n^{-1}. Solid circles show the experimental results for closed cavities of type *A* and open circles show the results for open cavities of type *D*. By the size of the circles the size of the cavities (3, 2, and 1 mm) is distinguished. Solid curves are predictions from the similarity model at $t=0.9$ ns with $S_s=5.0\times10^{12}$, 2.6×10^{13}, and 9.3×10^{13} W/cm^2 (from the lower to the upper curves). These vlaues for S_s are representative for the 3-, 2-, and 1-mm cavities.

9.3×10^{13} W/cm^2, i.e., with representative fluxes for the three types of cavities. S_s was calculated by using the same assumptions for $\eta_{\rm abs}$ and η_x as above. The results confirm basically the predicted reduction of the flux enhancement as the cavity is made more and more open. However, as noted already the flux enhancement is larger than predicted for the smallest cavities. This is particularly pronounced for the experiment with the 1-mm open (type-*D*) cavity.

With the help of Eq. (5) we can determine the quality factor N and the reemission coefficient r of the cavity wall. This determination involves the given fractional hole area n^{-1}, the incident laser flux $\bar{S}_L$, and assumptions about $\eta_{\rm abs}$ and η_x (in order to calculate S_s from $\bar{S}_L$), but no other assumptions about the physical mechanism of radiation confinement. With the assumptions for $\eta_{\rm abs}$ and η_x stated above, the highest value for N is bound for the 1-mm closed (type-*A*) cavity and amounts to $N=5.3$. The corresponding value for r is 0.84.

We have investigated [25] possible reasons for the larger than expected radiation in the experiment with the open 1-mm type-*D* cavity. One possibility suggested from this investigation is due to the fact that the expansion of the optically thick plasma from the radiatively heated wall into the cavity void leads to a reduction of the effective fractional hole area and hence the radiation loss through the hole is diminished with the consequence of higher temperature. However, such effects are multidimensional and are not easy to quantify. Because only a single experiment of this type was made and experimental errors cannot be excluded, we shall not discuss this point in more detail.

B. Comparison with numerical simulations

A more detailed comparison was made with numerical simulations by using the 1D hydrodynamic codes ILESTA [26] and MULTI [27]. These codes include multigroup radiation transport and nonlocal thermodynamic equilibrium (non-LTE) average ion model atomic physics. Specific problems were calculated by both codes and the results were checked for consistency. Because in the experiments the laser energy is deposited on a small fraction of the inner wall of the cavity, a concentric double-shell structure was adopted in order to model the experimental configuration. The inner sphere is irradiated by laser light. The radii of the inner and outer shells were so determined that the total area of both shells is equal to the area of the cavity used in the experiment and the area of the inner shell corresponds to the area on the wall of the experimental cavity which is irradiated by laser light. The radiation loss through the opening was taken into account by appropriate boundary conditions for the radiation fluxes at the outer and inner shells. The geometrical size of the cavity could be enlarged by a magnification factor M, i.e., M is the ratio for the cavity diameter adapted in the simulation to that for the experiment. Then the input energy was increased by a factor of M^2 in order to keep the laser irradiation intensity on the inner shell equal to the experimental value. If the cavity is scaled up in this way the plasma flow from the walls of the inner and outer shells approaches for large values of M a planar one and effects due to the finite size of the cavity (in particular the collision between the two plasmas produced at the inner and outer shells) are avoided, at least for a time of the laser pulse duration. The laser pulse shape given in Eq. (6) was used in the simulations.

Results from the simulations are shown in Figs. 7(a) and 7(c) together with the experimental results. The simulations were made with a magnification factor $M=100$, i.e., under conditions where no collision between the plasmas takes place during the observation time.

It may be noted from Fig. 7 that the similarity model (solid lines) and the simulations (open diamonds) give slightly different predictions. The more detailed simulations predict in general a somewhat lower reemitted flux than the similarity model, especially for a low incident laser flux (but the differences always remain below a factor of 2). The latter observation is not entirely unexpected and it may be attributed to the fact that for a low laser flux radiation and matter are not in complete thermodynamic equilibrium (as assumed in the similarity model). In this case the similarity model tends to overestimate the radiation flux and the simulation is expected to give a more realistic result (we note that equilibrium can be expected if $\hat{S}_{\rm hw}^2\hat{t}\geq0.1$ according to a recent comparison of the similarity model with simulations [28], and this criterion is represented by a boundary between the solid and dashed lines in Fig. 1). At the upper end of the considered range for the incident laser flux the simulation and the similarity model make very close predictions.

Now we consider the agreement between simulations and experiments. If one keeps in mind that the range

covered by the present experiments is very wide, the overall agreement is remarkably good. Considered in more detail, the experimental results give a somewhat higher reemitted flux at low incident laser fluxes than predicted by the simulation (and are, possibly accidentally, closer to the predictions of the similarity model). Such discrepancies raise questions about the accuracy of the opacity models used in the simulations and need further considerations. It is also seen from Fig. 7 that at the highest applied laser fluxes (i.e., in the 1-mm cavities) the measured flux tends to exceed the predicted flux. For example, in Fig. 7(a) the measured flux is higher by a factor of about 1.5 than predicted by the simulations; the same trend is seen in Fig. 7(c). With the help of simulations we investigated the possibility of whether additional heating could be due to effects connected with the finite size of the cavity, in particular the conversion of the kinetic energy of the expanding plasma (created mainly by laser light) into thermal radiation when the plasma collides in the center of the cavity. Simulations with $M=1$ have shown that additional heating of the cavity by this effect indeed occurs during the laser pulse and can lead to an increase of the flux in the cavity by a factor of about 1.5, but only for the 1-mm cavities. However, in quantitative

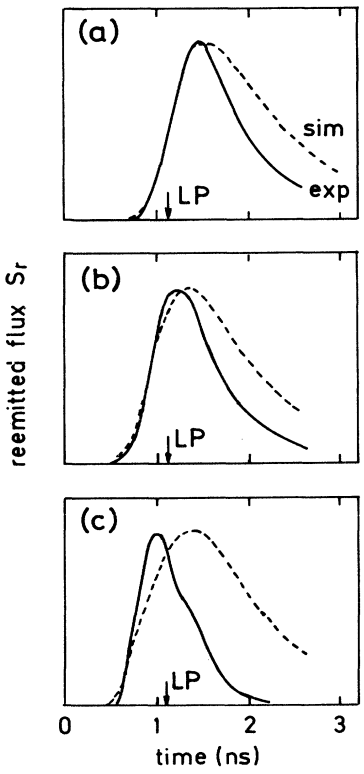

FIG. 9. Measured time history of reemitted radiation from (a) 3-mm, (b) 2-mm, and (c) 1-mm cavities of type A (solid lines) is compared with the results from the simulations (dashed lines). Curves are normalized to the same peak value. The vertical axis is in linear scale. The time of the laser peak is indicated by arrows.

respects, it remains open how accurately a spherical 1D code can model such filling effects by the laser-produced plasma which in reality originate in discrete areas on the cavity wall and expands in a more complicated manner. We note that a detailed computational study of the plasma collision effect on the reemitted radiation will be published elsewhere [25].

A comparison of the temporal behavior of the spectrally integrated reemitted flux is made in Fig 9. The peak values of the experimental and simulation results are all normalized to the same value. With respect to time the pulses have been layered upon each other in such a way that the maxima of the laser pulses in experiment and simulation coincide. The location of the laser-pulse maximum on the time scale was determined, in a previous experiment, from the maximum of x-ray emission from a uniformly heated spherical target where x-ray emission is known to follow closely the laser pulses. It is seen in Fig. 9 that the rising parts of the signals agree rather well with the simulation, at least for the 2- and 3-mm cavities. However, the simulated flux always decreases more slowly than the experimental one. It is basically unclear what causes this difference. But two remarks may be made in this respect.

(i) A similar difficulty is found in attempts to reproduce the time history of the x-ray signal from planar target experiments by simulation [29]. The fact that the experimentally observed x-ray signal tends to decay faster than in the simulation has been attributed to plasma cooling by lateral expansion which is not taken into account in 1D simulation. This may occur even in the cavity target because the laser heats only small spots in the cavity from which the plasma can expand laterally. Thus the source radiation in the experiment may decay faster than that reproduced by the simulation. Shortening of the source radiation leads to faster decay of reemitted radiation than calculated.

(ii) Another possible explanation is closure of the diagnostic hole by a plasma which evaporates from the edges of the hole and, due to its lower temperature, attenuates part of the radiation traversing the hole [30]. It is expected that this effect is most severe in the 1-mm cavities where the diagnostic holes are small and the plasma expansion velocity is high. In fact the measured duration of the x-ray signal (FWHM) for the 1-mm cavity [Fig. 9(c)] is only 0.67 ns (laser-pulse duration in this particular experiment was 0.86 ns) and the discrepancy to the simulation is largest. One might suspect that the hole closure effect increases towards the end of the laser light but the temporal effect is not well known. If attenuation should occur already at pulse maximum our measurements would underestimate the true flux inside the cavity. The possibility of hole closure certainly needs further investigation.

As already mentioned, simulations have shown that a plasma collision may occur in the center of the smallest (1-mm) cavity during the laser pulse and the reemitted radiation from the wall of the cavity is affected by reheating from the colliding hot plasma. Thus, under the present experimental conditions, the generation of intense radiation under clean conditions is possibly no longer main-

tained in the 1-mm cavity targets due to the presence of the stagnating plasma in the cavity.

V. SUMMARY

A detailed study of x-ray confinement in laser-heated cavities has been presented with measurements of x-ray emission from gold cavities heated by a high power 351-nm laser. At fixed laser energy (5 kJ) the brightness temperature of the radiation reemitted by the cavity wall rises with decreasing cavity size (i.e., with increasing laser intensity for heating). A maximum temperature of 240 eV and a reemission coefficient of 0.84 have been achieved for the smallest (1-mm) cavities used in the experiment. A net enhancement of the thermal radiation flux over the driving average laser flux found in this study indicates that the observed wall element is heated more by radiation from other wall elements than primary x-rays originating in the laser light. Evidence for confinement was also obtained from a comparison of radiation fluxes measured in the open and closed cavities.

It is shown that the experimental data covering a wide range of fluxes are in general well predicted by the scaling laws derived from a similarity model, based on the self-similar solution for the ablative heat wave in the wall of the cavity. This indicates that the model describes radiation confinement correctly and therefore can be a useful tool for predicting radiation fluxes in various types of cavities. We have also simulated the experiments in more detail with 1D radiation hydrodynamic codes. It is found that the cavity radiates for a somewhat shorter time than predicted which is possibly a consequence of diagnostic hole closure with plasmas. The simulations also suggest that in the smallest (1-mm) cavities the temperature may be slightly enhanced due to radiation emission by an imploding and stagnating plasma in the center of the cavity. Such effects need further consideration if one is interested in generating the highest possible temperature with a given laser power.

ACKNOWLEDGMENTS

The authors gratefully acknowledge the help and support provided by many people throughout the progress of this work. We appreciate the assistance of laser operation, target fabrication, and data acquisition provided by the members of Institute of Laser Engineering, Gekko operation and device, measurement, target, and optical technology groups and Max-Planck-Institut für Quantenoptik laser-plasma group. This work was supported in part by the Commission of the European Communities in the framework of the Euratom-IPP Association and by Monbusho International Scientific Research Program.

*Present address: Institute for Laser Technology, 1-8-4 Utsubohonmachi, Nishiku, Osaka 560, Japan, and Himeji Institute of Technology, Himeji, Hyogo, 671-22, Japan.

†On leave from: Institute of Laser Engineering, Osaka University, Suita, Osaka 565, Japan.

‡On leave from: Department of Electrical Engineering, University of Alberta, Edmonton, Alberta, Canada T6G 2G7.

[1] R. Pakula and R. Sigel, Phys. Fl. **28**, 232, (1985); **29**, 1340 (E) (1986).

[2] R. E. Marshak, Phys. Fl. **1**, 24 (1958).

[3] G. D. Tsakiris and K. Eidmann, J. Quantum Spectrosc. Radiat. Trans. **38**, 353 (1987).

[4] S. Sakabe, R. Sigel, G. D. Tsakiris, I. B. Földes, and P. Hermann, Phys. Rev. A **38**, 5757 (1988).

[5] G. D. Tsakiris and R. Sigel, Phys. Rev. A **38**, 5767 (1988).

[6] R. Sigel, R. Pakula, S. Sakabe, and G. D. Tsakiris, Phys. Rev. A **38**, 5779 (1988).

[7] T. Mochizuki, T. Yabe, H. Azechi, K. A. Tanaka, T. Boehly, N. Miyanaga, H. Nishimura, S. Ido, M. Yamanaka, K. Mima, S. Naki, C. Yamanaka, R. Sigel, G. D. Tsakiris, K. Eidmann, P. Hermann, R. Pakula, S. Sachsenmaier, S. Sakabe, and S. Witkowski, in *X-ray Confinement in a Laser-Heated Cavity,* Proceedings of the 11th International Conference on Plasma Physics and Controlled Nuclear Fusion Reasearch, Kyoto (IAEA, Vienna, 1987), Vol. 3, p. 25.

[8] K. Kondo, H. Nishimura, T. Endo, H. Shiraga, T. Yabe, Y. Kato, and S. Nakai, in *Behavior of Soft X-ray Emitting Plasmas in Cannonball Targets and their Emission Properties,* edited by C. Yamanaka, Springer Proceedings in Physics Vol. 30 (Springer-Verlag, Berlin, 1988).

[9] K. Kondo, H. Nishimura, H. Sakurai, K. Nishihara, Y. Izawa, Y. Kato, C. Yamanaka, and S. Nakai, Jpn J. Appl. Phys. **28**, 1695 (1989).

[10] H. Nishimura, H. Azechi, M. Nakai, S. Uchida, Y. Sakawa, T. Wada, H. Hasegawa, H. Sakurai, T. Yamanaka, and C. Yamanaka, Opt. Commum. **56**, 409 (1986).

[11] Y. Sakawa, K. A. Tanaka, H. Nishimura, M. Nakai, T. Yabe, H. Sakurai, Y. Izawa, Y. Kato, T. Mochizuki, M. Nakatsuka, and C. Yamanaka, Phys. Fluids **30**, 3276 (1987).

[12] I. B. Földes, R. Sigel, Chen Shi-sheng, K. Eidmann, R. F. Schmalz, G. D. Tsakiris, and S. Witkowski, Laser Part. Beams **6**, 123 (1988).

[13] P. D. Goldstone, S. R. Goldman, W. C. Mead, J. A. Cobble, G. Stradling, R. H. Day, A. Haner, M. C. Richardson, R. S. Majoribanks, P. A. Jaanimagi, R. L. Keck, F. J. Marshall, W. Seka, O. Barnouin, B. Yaakobi, and S. A. Letzring, Phys. Rev. Lett. **59**, 56 (1987).

[14] H. Nishimura, H. Takabe, K. Kondo, T. Endo, H. Shirage, K. Sugimoto, T. Nishikawa, Y. Kato, and S. Nakai, Phys. Rev. A **43**, 3073 (1991).

[15] R. Sigel, G. D. Tsakiris, F. Lavarenne, J. Massen, R. Fedosejevs, J. Meyer-ter-Vehn, M. Murakami, K. Eidmann, S. Witkowski, H. Nishimura, Y. Kato, H. Takabe, T. Endo, K. Kondo, H. Shirage, S. Sakabe, T. Jistuno, M. Takagi, C. Yamanaka, and S. Nakai, in *Heat Wave and Radiation Confinement in Laser-heated Cavities,* Proceedings of the 13th International Conference Plasma Physics and Controlled Nuclear Fusion Research (IAEA, Washington, DC, 1990), IAEA-CN-53/B-2-1 (unpublished).

[16] R. Sigel, in *Laser Generated Intense Thermal Radiation* edited by M. N. Rosenbluth and R. Z. Sagdeev, Handbook of Plasma Physics Vol. 3, and *Physics of Laser Plasma,* edited by S. Witkowski and A. Rubenchik (North-Holland, Amsterdam, 1991).

[17] C. Yamanaka, Nucl. Fusion **25**, 1343 (1985).
[18] G. D. Tsakairis, J. Massen, R. Sigel, F. Lavarenne, R. Fedosejevs, J. Meyer-ter-Vehn, K. Eidmann, H. Nishimura, Y. Kato, H. Takabe, T. Endo, K. Kondo, H. Shiraga, S. Sakabe, T. Jitsuno, M. Takagi, C. Yamanaka, and S. Nakai, Phys. Rev. A **42**, 6188 (1990).
[19] R. Sigel, G. D. Tsakiris, F. Lavarenne, J. Massen, R. Fedosejevs, J. Meyer-ter-Vehn, M. Murakami, K. Eidmann, S. Witkowski, H. Nishimura, Y. Kato, H. Takabe, T. Endo, K. Kondo, H. Shiraga, S. Sakabe, T. Jitsuno, M. Takagi, C. Yamanaka, and S. Nakai, Phys. Rev. Lett. **65**, 587 (1990).
[20] R. Sigel, G. D. Tsakiris, F. Lavarenne, J. Massen, R. Fedosejevs, K. Eidmann, J. Meyer-ter-Vehn, M. Murakami, S. Witkowski, H. Nishimura, Y. Kato, H. Takabe, T. Endo, K. Kondo, H. Shiraga, S. Sakabe, T. Jitsuno, M. Takagi, S. Nakai, and C. Yamanaka, Phys. Rev. A (to be published).
[21] H. W. Schnopper, P. L. van Speybroeck, J. P. Delvaille, A. Epstein, E. Källne, R. Z. Bachrach, Y. H. Dijkstra, and L. Lantward, Appl. Opt. **16**, 1088 (1977).
[22] K. Eidmann, K. Kühne, P. Müller, and G. D. Tsakiris, J. X-Ray Sci. Technol. **2**, 259 (1990).
[23] K. Eidmann, T. Kishimoto, P. Hermann, J. Mizui, R. Pakula, R. Sigel, and S. Witkowski, Laser Part. Beams **4**, 521 (1986).
[24] W. Schwanda and K. Eidmann, Appl. Opt. (to be published).
[25] J. Massen, Ph.D. dissertation, Ludwig-Maximilians Universität, München, 1991.
[26] H. Takabe, M. Yamanaka, K. Mima, C. Yamanaka, H. Azechi, N. Miyanaga, M. Nakatsuka, T. Jitsumo, T. Norimatsu, M. Takagi, H. Nishimura, M. Nakai, T. Yabe, T. Sasaki, K. Yoshida, K. Nishihara, Y. Kato, Y. Izawa, T. Yamanaka, and S. Nakai, Phys. Fl. **31**, 2884 (1988).
[27] R. Ramis, R. Schmalz, and J. Meyer-ter-Vehn, Comp. Phys. Commun. **49**, 475 (1988).
[28] M. Murakami and J. Meyer-ter-Vehn, Nucl. Fusion **31**, 1315 (1991).
[29] W. C. Mead, E. K. Stover, R. L. Kauffman, H. N. Kornblum, and B. F. Lasinski, Phys. Rev. A **38**, 5275 (1988).
[30] R. L. Harrach, Rev. Sci. Instrum. **57**, 2192 (1986).

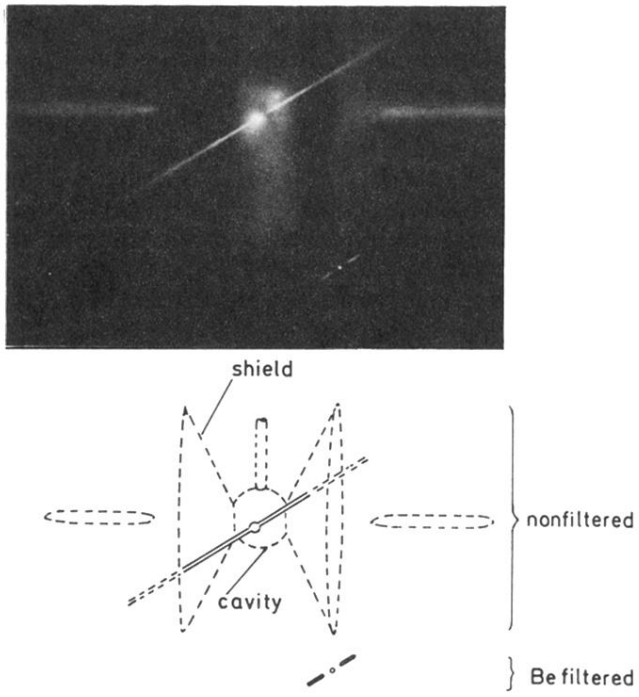

FIG. 4. A typical film image from TGS equipped with two pinhole gratings. The two spectra from the unfiltered (upper) and filtered (lower) pinhole gratings are superimposed on a pinhole image of the radiating cavity, produced in zeroth order by the unfiltered grating. Dispersion direction of the grating was tilted in order to avoid the spectra coinciding with the radiating plasma jets from the shields.